PCCP

View Online
Dynamic Article Links

Cite this: DOI: 10.1039/c0cp02359k

www.rsc.org/pccp

PERSPECTIVE

Optical fluid and biomolecule transport with thermal fields

Franz M. Weinert, Christof B. Mast and Dieter Braun*

Received 2nd November 2010, Accepted 8th December 2010
DOI: 10.1039/c0cp02359k

Published on 17 January 2011 on http://pubs.rsc.org | doi:10.1039/C0CP02359K
Downloaded by Ludwig Maximilians Universitaet Muenchen on 24 January 2011

A long standing goal is the direct optical control of biomolecules and water for applications ranging from microfluidics over biomolecule detection to non-equilibrium biophysics. Thermal forces originating from optically applied, dynamic microscale temperature gradients have shown to possess great potential to reach this goal. It was demonstrated that laser heating by a few Kelvin can generate and guide water flow on the micrometre scale in bulk fluid, gel matrices or ice without requiring any lithographic structuring. Biomolecules on the other hand can be transported by thermal gradients, a mechanism termed thermophoresis, thermal diffusion or Soret effect. This molecule transport is the subject of current research, however it can be used to both characterize biomolecules and to record binding curves of important biological binding reactions, even in their native matrix of blood serum. Interestingly, thermophoresis can be easily combined with the optothermal fluid control. As a result, molecule traps can be created in a variety of geometries, enabling the trapping of small biomolecules, like for example very short DNA molecules. The combination with DNA replication from thermal convection allows us to approach molecular evolution with concurrent replication and selection processes inside a single chamber: replication is driven by thermal convection and selection by the concurrent accumulation of the DNA molecules. From the short but intense history of applying thermal fields to control fluid flow and biological molecules, we infer that many unexpected and highly synergistic effects and applications are likely to be explored in the future.

I. Introduction

Optical methods of manipulating and investigating matter have unique advantages[1] and are present all over the life sciences.[2] While high confinement of optical resolution can be used for photolithography to pattern materials without physical contact at an ever increasing level of miniaturization,[3] optical tweezers use the momentum transfer of light to remotely move microscale objects. Although the whole range of its applicability was not obvious in the beginning,[4] this technique was developed to a sensitive force sensor for single molecules, which had an enormous impact in molecular biology.[2,5]

Furthermore, handling of liquids on the microscale became an important topic in the past, especially in the life sciences, since it shortens the time of the experiment, enhances the signal to noise ratio of detection and reduces the overall consumption of chemicals and labor. Several ways to remotely switch valves in micromanufactured channels for the control of fluid flow in channels have been explored.[6–10] Optical methods have been investigated to move covered liquid droplets[11,12] or to drive liquid flow by holographically induced vortex flows near trapped particles.[13] Lithographic surface patterning is used to induce droplet movement by thermo-capillary actuation[14] or surface acoustic waves.[15] Here we review a set of recently developed methods which uses optically created temperature fields to generate arbitrary flow patterns of liquids, to move and trap solved biomolecules down to the size of a few nanometres and to manipulate and analyze biomolecules in free solution or in their natural environment, the living cell. The optical control of temperature enables arbitrary temperature jumps within hundreds of microseconds and spatial resolution in the micrometre range. The amplitude of the temperature jump depends on the laser power and the absorption coefficient of the used wavelength. It is not coupled to the raise time. In general it can be arbitrary, *i.e.* from the ambient temperature up to the boiling temperature of the used liquid. This allows for measuring DNA melting curves in milliseconds, setting up ideal conditions for enzymes or performing thermal cycling for PCR reactions. Since all techniques are driven by the same optical setup, they can be combined arbitrarily.

The thermal movement of molecules is an unexpected effect. We only slowly learn more about why molecules exactly move in a thermal gradient. While it can be argued that the magnitude of the effect is small, recent advances showed that it is especially useful in the characterization of biomolecular

Systems Biophysics, Center for Nanoscience, Physics Department, Ludwig Maximilians Universität München, Amalienstr. 54, 80799 München, Germany. E-mail: dieter.braun@lmu.de

View Online

Downloaded by Ludwig Maximilians Universitaet Muenchen on 24 January 2011
Published on 17 January 2011 on http://pubs.rsc.org | doi:10.1039/C0CP02359K

binding in its native environment. To understand this, we have to compare the thermal movement—named thermophoresis, thermal diffusion or Soret effect—with the well known method of electrophoresis.

Electrophoresis is extensively used in biology, however it has significant and important drawbacks. Generally, electrophoresis gels have to be used to gain a size selective electrophoretic movement. Without them, typical biological molecules move in an electrical field with equal velocity. Thus, electrophoresis has to use a special matrix and special buffers, making it impossible to analyze biomolecules in their native environment.

Although the speed of thermophoresis is typically well below 1 μm s^{-1}, its unique surface sensitivity under complex buffer conditions and the possibility to miniaturize the approach using an all-optical fluorescence detection and infrared heating technique made thermophoresis a very useful technique in the detection of biomolecular binding.

II. Light driven microfluidics in water

In this section we describe a technique to generate and control an arbitrary flow pattern in any thin liquid layer by the repetitive movement of a focused infrared laser. The laser is used to generate temperature changes in micrometre thin water layers (Fig. 1a). Due to fast thermal coupling to the near glass windows, temperature spots can be generated with diameters of only a few micrometres and changed with rates faster than 10 kHz. As a result, the water in the wake of the spot cools down very fast when the heating laser spot is moved through the liquid layer. The result is a spatially symmetric moving warm spot. If the spot speed does not allow for full equilibration of the temperature, *i.e.* for velocity larger than the spot diameter divided by the thermal equilibration time, the temperature spot becomes elongated and is followed by an exponentially decaying temperature tail. Consider the spot is moving towards the left (Fig. 1b). The water in front of the spot heats up while the water in the wake of the spot cools down to ambient temperature again. The resulting density changes of the water lead to divergent flows due to mass conservation.[16] In front of the spot the water expands, while in the wake it contracts again. At constant viscosity the system is symmetric and the contraction exactly cancels out the previous expansion. However, the temperature dependence of the viscosity breaks the symmetry. A lower viscosity at higher temperatures for example increases the velocities in the warm spot between the expansion and contraction (see bottom of Fig 1b). The result is a net flow against the spot direction. When the spot passes over once, the net shift of the water after expansion and successive contraction is in the tens of nanometre scale. However, the laser movement can be repeated in the kHz regime due to the fast thermal coupling to the nearby glass windows. Therefore reasonable fast pumping velocities in the order of 100 μm s^{-1} can be achieved, generated and defined by the movement of the laser.

Using the nonlinear effect described here, we can, for example, move water along the letters "LASER PUMP" without lateral walls to guide the flow (Fig. 2). In the experiment, we sandwich a 10 μm thin sheet of water between glass slides and move a focused infrared laser along the letters. The water is locally heated by direct absorption of the laser irradiation. The spot movement along the letters is repeated in the kilohertz regime. As a result, the fluid flows in the reverse path of the warm spot movement.

To test the model of thermally induced asymmetric expansion, a finite element simulation of the three dimensional Navier–Stokes equation was performed (Fig. 3a). The system of interest allows to do a set of approximations. We can for example assume the flow to be laminar and therefore neglect the inertia terms. Furthermore dimensions parallel to the surface are much greater than the width of the water layer, which allows us to do a thin film approximation and describe the system as a two-dimensional flow (Fig. 3b). By further approximation, which can be tested by the finite element simulations (for details see ref. 16–18), it is possible to obtain

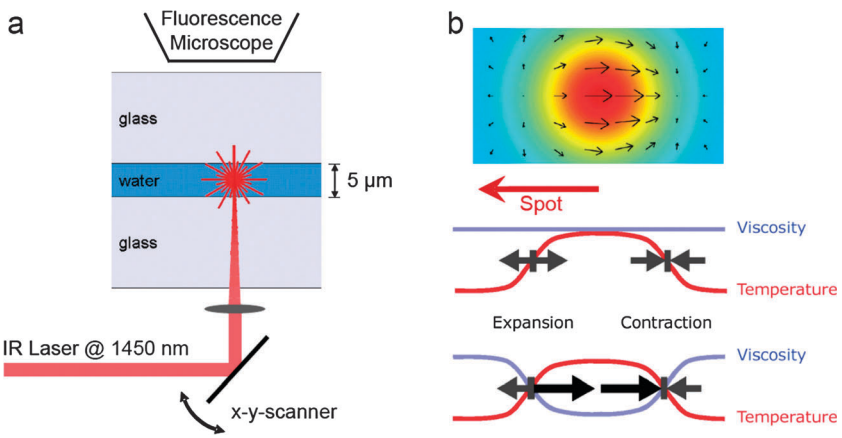

Fig. 1 (a) Schematic view of the experimental setup. An infrared laser is deflected by an Acousto-Optical Deflector and focused into a thin water layer between two glass windows. The water absorbs a part of the light. The result is a spot of raised temperature localized at the optical focus of the laser. (b) Moving the warm spot generates local fluid flows due to density changes of the water. The water expands in the front of the spot and contracts again in the wake. At constant viscosity both movements cancel out one another. However, the lower viscosity of the liquid at higher temperatures leads to increased velocities inside the warm spot. The result is a net flow against the spot direction. [Copyright *Journal of Applied Physics*].

This journal is © the Owner Societies 2011

View Online

Downloaded by Ludwig Maximilians Universitaet Muenchen on 24 January 2011
Published on 17 January 2011 on http://pubs.rsc.org | doi:10.1039/C0CP02359K

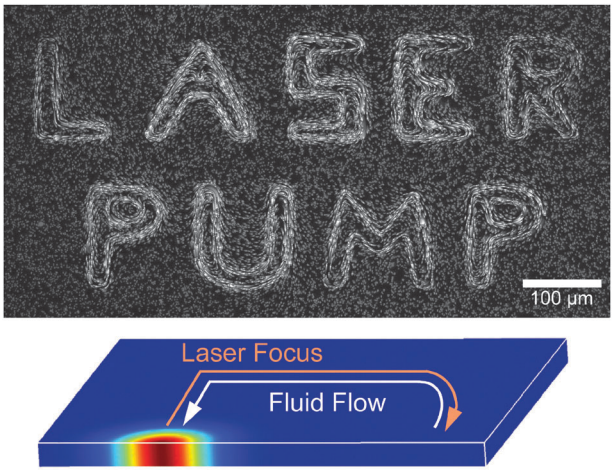

Fig. 2 Pumping water optically along arbitrary patterns. Fluid flow along the letters "LASER PUMP" is driven by dynamically heating a thin fluid film with a laser scanning microscope. As seen, complex flow patterns are easily accomplished. No channels restrict the fluid flow. Local pumping of the fluid film is the result of thermoviscous fluid movements for each passage of the laser focus. We visualize the water flow by fluorescent tracer particles. [Copyright *Journal of Applied Physics*].

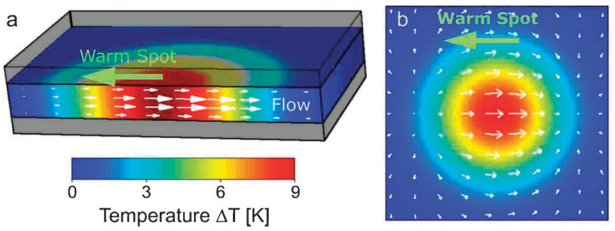

Fig. 3 Finite element simulation of the Navier–Stokes equation in the frame of reference of the moving spot. (a) Three dimensional calculation. (b) The model can be reduced to 2 dimensions by making a thin film approximation. [Copyright *Journal of Applied Physics*].

an analytical formula, which describes the pump velocity under a set of parameters:

$$v_{\mathrm{pump}} = -\frac{3\sqrt{\pi}}{4} f \alpha \beta b \Delta T^2, \qquad (1)$$

where f is the repetition frequency of the laser, α is the expansion coefficient, β is the temperature dependence of the viscosity, b is the spot width and ΔT is the amplitude of the temperature in the spot. The temperature can be obtained by imaging a temperature sensitive fluorescent dye added to the water. The shape of the moving warm spot is measured by stroboscopic illumination with a LED using a 10 µs long rectangular light pulse each time the laser spot passes by.

Since all parameters used in eqn (1) can be measured, the theoretical formula can be tested without fitting parameters. Every passage of the warm spot results in a liquid step Δx opposite to the spot movement direction. The pump speed is therefore expected to increase in a linear fashion with repetition frequency of the laser spot as given by eqn (1). This predicted behavior can be verified by measurements in the low frequency regime $f \ll 1$ kHz as shown in the inset of Fig. 4a. The repetition rate f in this experiment was adjusted by moving the laser spot with increased velocity along a fixed circular pump geometry. For slow frequencies, the spot temperature distribution remains in its Gaussian shape. However, a further increase in the spot velocity results in a considerable elongated temperature spot geometry which enhanced the pump speed beyond the linear estimate for constant spot width b (Fig. 4a). Examples of spot geometries as measured with stroboscopic temperature imaging are given as color coded insets. Interestingly, the enhanced pump velocity at high laser spot velocities could still be described when the elongated temperature spot geometry was taken into account with a spatial integral of eqn (1) for each repetition rate (Fig. 4a, solid line).

The analytical theory predicts a linear response of the pump velocity to both the thermal expansion $\alpha \Delta T_0$ and the change in

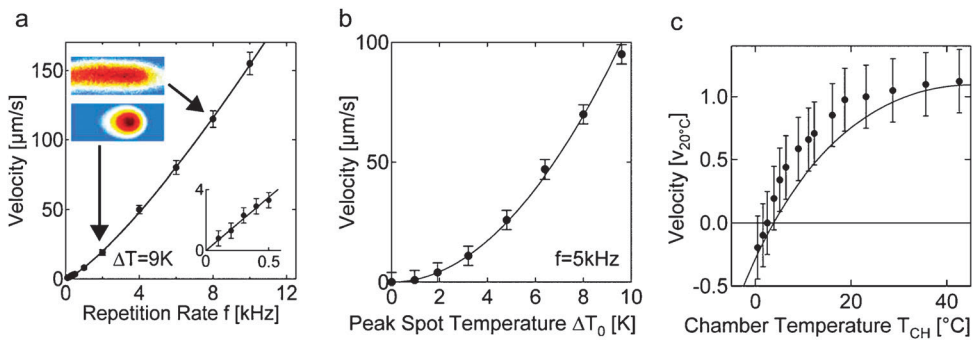

Fig. 4 Testing and comparing the analytical formula with measured pump velocities. (a) The pump velocity is a linear function of the repetition rate for $f = 1$ kHz when the spot geometry remains Gaussian. (inset: temperature image). At faster rates, the warm spot becomes elongated due to the finite thermal equilibration time of cooling. Accordingly, the pump velocity is enhanced beyond the linear prediction as the spot width b increases from 10 to 20 µm in the 5 µm thin fluid film. The solid line predicts the pump velocities based on extrapolated temperature profiles for each repetition rate f. (b) The pump velocity rises with the square of the spot temperature, confirming the linear dependence on both the thermal expansion and the temperature dependence of the viscosity. Pump velocities are predicted by eqn (1) without fitting parameters at a spot width $b = 25$ µm. (c) By changing the overall chamber temperature, we can probe the dependence on thermal expansion and temperature dependent viscosity. At 4 °C, the water contracts upon heating. As expected from eqn (1), pump velocity reverses its direction (solid line). In all plots, error bars show standard errors from particle tracking. [Copyright *Journal of Applied Physics*].

View Online

the temperature dependent viscosity $\beta\Delta T_0$ for a similar shape of the temperature spot. If the spot temperature is enhanced by higher laser power, the pump velocity increases proportionally to ΔT_0^2 as shown in Fig. 4b. The solid line results from eqn (1) without additional fitting parameters. The proportionality to the parameters α and β is tested by changing the ambient temperature T_{ch} of the chamber. In Fig. 4c we changed T_{ch} by cooling the microscope stage with an external heat bath. The experiments reveal a reversal of the pump direction at fluid temperatures below 4 °C. We attribute this reversal to the sign change of the volume expansion coefficient α. Again the theoretical expectation of eqn (1) fits the experimental pump velocities.

While the dynamic control of fluid flow on the micrometre scale is an interesting subject by itself, the capability to transport dissolved molecules is crucial for microfluidic applications. Traditional microfluidics use micromachined channels to hinder diffusion of molecules perpendicular to the pump direction. While our technique can also pump along such optically transparent channels, we aim at more flexible and previously impossible settings. For example, the method allows the usage of unstructured and disposable chambers.

To show that light driven pumping can be used in microfluidic applications, we demonstrate a purely light driven fluid mixer for small biomolecules. The initial condition is prepared by sandwiching two droplets containing initially warm low melting temperature agarose gel between glass slides. One droplet additionally contains a fluorescent labeled biomolecule. After covering the droplets by the glass slide, the droplets spread out and form an interface between one another (Fig. 5). The laser pump can be used to transport the fluorescent molecules into three pockets of different areas and mixed with the surrounding dark liquid with volume ratios of 4 : 1, 1 : 1 and 1 : 4.

III. Light driven microfluidics in ice

While the above approach works well for particles or long bio-molecules, small molecules can still diffuse through the gel and cannot be confined by the channels. In the following we will show that ice sheets can be used instead of gels to hinder diffusion. The infrared laser could be used to melt channels filled with liquid water into the ice. This system becomes even more interesting, when the channel freezes again behind the

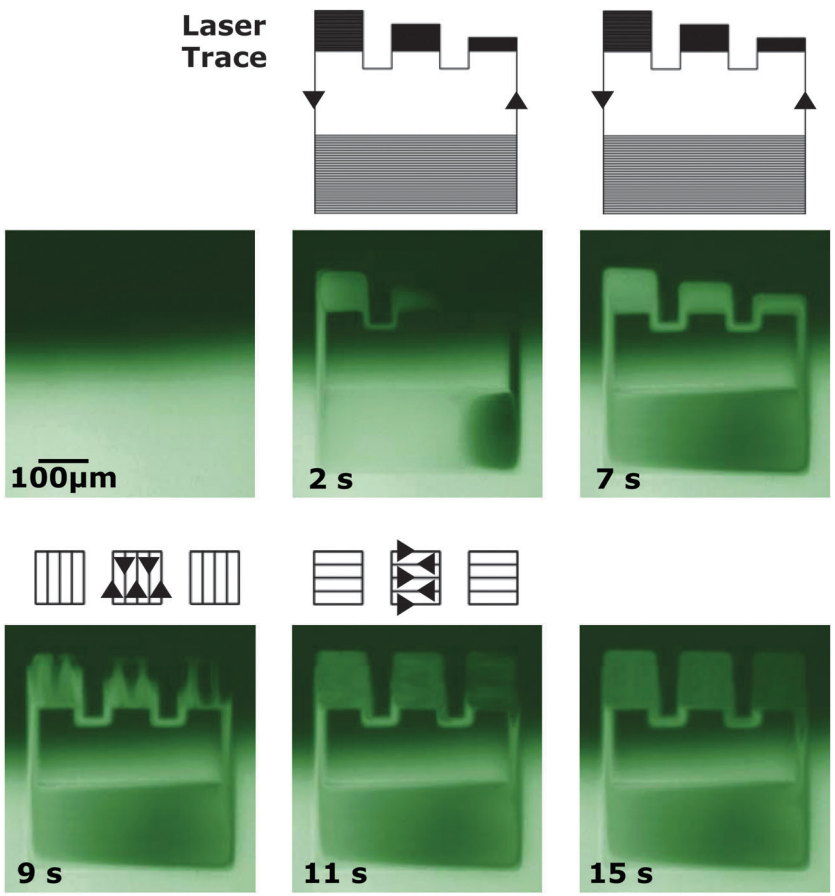

Fig. 5 Fast light driven creation of a dilution series. We have created an interface between two neighboring gels with no biomolecules on top and with biomolecules at the bottom. The stained biomolecules are first driven optically to three chambers to the top and mixed with different volumes of buffer. The result is a dilution series only created by optical fields. First, three volumes of 65, 40, and 20 pl are created with the laser pattern shown above the fluorescence images. Note that the laser direction is opposite to the pump direction. In a second step the fluid is mixed by repeatedly pumping rectangular ring flows with perpendicular orientation. The result is a dilution series with volume ratios of 4 : 1, 1 : 1, and 1 : 4 in equal volumes. [Copyright *Journal of Applied Physics*].

Downloaded by Ludwig Maximilians Universitaet Muenchen on 24 January 2011
Published on 17 January 2011 on http://pubs.rsc.org | doi:10.1039/C0CP02359K

 This journal is © the Owner Societies 2011

View Online

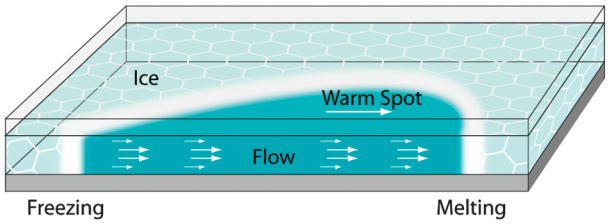

Fig. 6 An optically created temperature spot is moved to the right in a sheet of ice. The ice melts in front of the spot (right) and freezes behind it (left) and moves the fluid due to the difference in specific volume. [Copyright *Applied Physics Letters*].

heating laser spot, rather than remaining permanently thawed. By repeating the laser spot movement, the water undergoes a series of melting and freezing circles. At high repetition frequencies, considerably faster pump velocities can be achieved.[18]

The principle works as follows. Consider a spot of enhanced temperature, induced by the focused infrared laser, moving through a thin ice sheet (Fig. 6). The ice thaws at the front of the spot and freezes in its wake. The density change during the phase transition induces divergent flows due to mass conservation, with a sink (div $v > 0$) at the front and a source (div $v < 0$) at the back. The solid ice boundaries force the direction of the liquid movement towards the front of the molten compartment. We assume a parabolic flow profile perpendicular to the glass/silicon boundaries with $v_{avg} = 2/3 v_{water}$, where v_{water} is the peak velocity in the center of the fluid sheet. With the continuity equation ρ at the water–ice boundary, d_{spot} denoting the end to end distance of the molten area and if the spot movement is repeated with frequency f, we expect a pump velocity

$$v_{pump} = \Delta x f = \frac{3}{2}\frac{\rho_{water} - \rho_{ice}}{\rho_{water}} d_{spot} f. \qquad (2)$$

The length of the moving spot d_{spot} can be measured by stroboscopic white light imaging. A typical image of the drop-shaped molten area with $d_{spot} = 120$ μm is shown in Fig. 7c. For example for a repetition rate of $f = 650$ Hz with densities $\rho_{water} = 1000$ kg m^{-3} and $\rho_{ice} = 917$ kg m^{-3} we expect $v_{pump} = 9.5$ mm s^{-1}. Experimentally, we find 11 mm s^{-1} which is in agreement with the theoretical expectations.

The length of the molten spot depends on the temperature of the ice sheet (Fig. 7b). At low ice temperatures, only a short spot is molten. At higher ice temperatures, the molten spot can reach lengths beyond 500 μm with the pump velocity exceeding 50 mm s^{-1} (Fig. 7a). With this dependence, theory and experiment match quantitatively. For further increased chamber temperatures, the front of the thawed spot catches up with the back of the previous heating cycle which results in thermoviscous pumping in the reverse direction as described above. To conclude, we expect that the repetitive melting–freezing cycles are not very stressful to biomolecules since ice, if cooled as in our case on the millisecond time scale, remains amorphous and without grain boundaries.

IV. Thermophoresis: from fundamentals to binding assays

Thermophoresis is the movement of molecules in a static thermal gradient. So far, we have seen, how a dynamic thermal warming allows the fluid to move. In the following section, we will discuss how a static thermal gradient moves molecules. Already from this onset, it should be clear that we will be able to combine thermophoretic movement with fluid movement in an almost arbitrary manner as the dynamic and static thermal fields can be superposed with great flexibility.

The optical detection and induction of molecule movement in a thermal gradient is interesting from a fundamental point of view. Many more experiments have to be performed to completely understand the microscopic effects which drive the molecules in a thermal gradient. Equally interesting is the application of thermophoresis in biology, which was first demonstrated only a year ago by measuring binding curves between biologically relevant binding partners.[19,20]

We can only give a short and very rough overview over the fast growing field here. In the past many researchers have used optical density as detection for thermophoresis.[21–26] Since the signal is weak, rather high concentrations have to be employed and rather complex detection methods established to obtain enough signal. Examples are methods of beam deflection,[21,24] thermal lensing,[25] electrical heating[26] and holographic gratings with heterodyne detection approaches.[22,23]

In contrast, we have argued that the addition of a fluorescent marker to the molecule under consideration is a big advantage. Typically, the size of the marker does not change the thermophoretic properties significantly and moreover, for the study of fundamental aspects, the staining can be tuned to not affect the desired question at hand. For example, DNA can be end

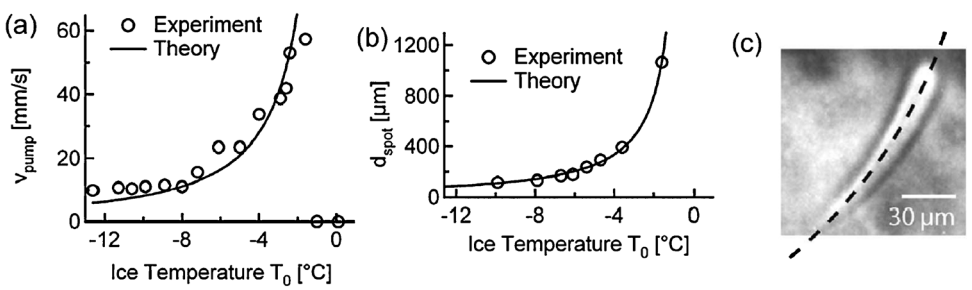

Fig. 7 (a) Pump velocities depend on the ice temperature T_0 (open circles). Eqn (2) predicts the pump velocity. (b) The length of the thawed spot becomes more elongated for higher T_0. (c) Stroboscopic image of the molten spot along a circular path, shown by the broken line. [Copyright *Applied Physics Letters*].

Downloaded by Ludwig Maximilians Universitaet Muenchen on 24 January 2011
Published on 17 January 2011 on http://pubs.rsc.org | doi:10.1039/C0CP02359K

View Online

Downloaded by Ludwig Maximilians Universitaet Muenchen on 24 January 2011
Published on 17 January 2011 on http://pubs.rsc.org | doi:10.1039/C0CP02359K

labeled, changing the overall charge and size of the molecule by less than 5%.

On the other side we gain two very important aspects. First, specificity: the marker enables us to measure the molecule in very complex mixtures and thus allows testing the fundamental aspects under a wide variety of buffer conditions. This becomes fundamental for the detection of molecule binding in for example blood serum.[19,20] Second, sensitivity: fluorescence allows us to detect the motion of attomolar concentrations for larger particles and typically reaches low nanomolar concentrations of biomolecules such as DNA or proteins with a single marker. Methods using refractive index as proxy do not reach such sensitivities. Fluorescence, one should mention, even allows tracking of individual particles in a thermal gradient.[27,29]

As fluorescence is an imaging technique with high sensitivity, we have direct control over fluid dynamics artifacts such as convection and can easily monitor binding of the molecules to surfaces or the formation of molecule clusters.

As it can be combined easily with optical temperature control, fluorescence imaging gives even more freedom in designing the experiments. For example, the DNA concentration can be imaged by fluorescence, while it is structured by optical temperature patterning along letters in a thin fluid film[27] (Fig. 8a) or imaged after the DNA has accumulated in microfluidic channels as thermophoresis and flow compete[28] (Fig. 8b). Thermophoretic flow around large particles[29] or the combined accumulation of DNA by convection and thermophoresis can be easily shown.[30,31] One nice case of how fluorescence allows the recording of complex phenomena is measurements where the competing depletion of a high concentration molecular crowding agent reverses the thermophoretic direction and inverts a depletion to an attraction.[32]

Due to space limitations we can't go into the details of possible explanations of thermophoresis. Basically, the experiments are tried to be described with two competing approaches. One argues that thermophoresis is a movement with low Peclet number and is more a biased diffusion motion than a directed motion. As a result, it is argued, the effect is dominated by a local thermodynamic equilibrium. Experiments support this view and demonstrate a description of thermophoresis in its size and salt dependence without fit parameters for both polystyrene beads and DNA.[27,33] Conversely competing size dependencies have been measured with different geometries, particles and methods,[27,34] without however recording the salt dependence. Whether the difference is an effect of electrical fields built up by the thermophoresis of ions,[35,36] or of the differing heating from surfaces or free fluid has to be investigated in the future. What appears clear is that when the thermal gradient grows to the extent that the Peclet number is larger than one and the movement is ballistic, Maragoni-like fluid patterns emerge and particles show hydrodynamic attraction.[29]

The speed of thermophoretic movement in typical temperature gradients of less than 0.1 K μm^{-1} is typically well below 1 $\mu m\ s^{-1}$, many order of magnitudes slower than electrophoresis. Nevertheless, the inherent size selectivity of the effect and its unique sensitivity to interfacial properties of the molecule–water interface makes it a very sensitive tool to detect changes of molecules where the diffusion coefficient or an electrophoretic movement does not record a change of the molecule. This means that thermophoresis will not be able to be used for the separation of a molecule mixture into bands of different size. However the most important biological questions do not require such separation capability. The binding of molecules, *i.e.* the analog of gel shift assays, can be handled with exquisite precision with the thermophoretic approach.

What came to the attention only recently is the use of thermophoresis for the analysis of biomolecule affinity and activity. The approach has been in the meanwhile commercialized by NanoTemper Technologies. By using capillaries, fluorescence labeling and infrared heating, a robust platform is obtained which is very flexible in a wide variety of biological settings. Here we only want to give one example which is particularly promising for the evaluation of pharmaceutical compounds (Fig. 9).[20]

Kinases are an important target for pharmaceuticals as they are the backbone of cellular signaling and play an important role in many diseases. The search of inhibitors is thus very important for the pharmaceutical industry. However the size difference between the protein (typically 40 kDa) and the inhibitor (typically 0.5 kDA) is big and makes the detection of binding with diffusion-based techniques such as FCS impossible. Also the dual labeling of the small compounds is in most cases prohibitive. However, although it was initially unexpected, thermophoresis can detect the binding by the thermophoretic depletion of the protein. It is only required to finetune the measurement conditions to allow a highly reproductive and precise measurement of thermophoresis.[20]

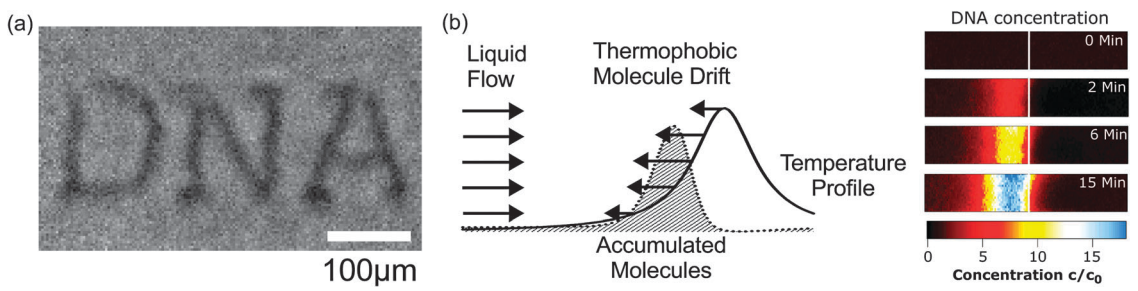

Fig. 8 (a) Thermophoresis. DNA moves form the warm to the cold region, visualized by the optical heating of the letters "DNA" and fluorescence imaging of the DNA concentration. [Copyright Proceedings of the National Academical Society, USA]. (b) Combination of thermophoresis with a flow in a microchannel leads to the accumulation of DNA at the upflow position of the heating spot. [Copyright *Physical Review Letters*].

 This journal is © the Owner Societies 2011

View Online

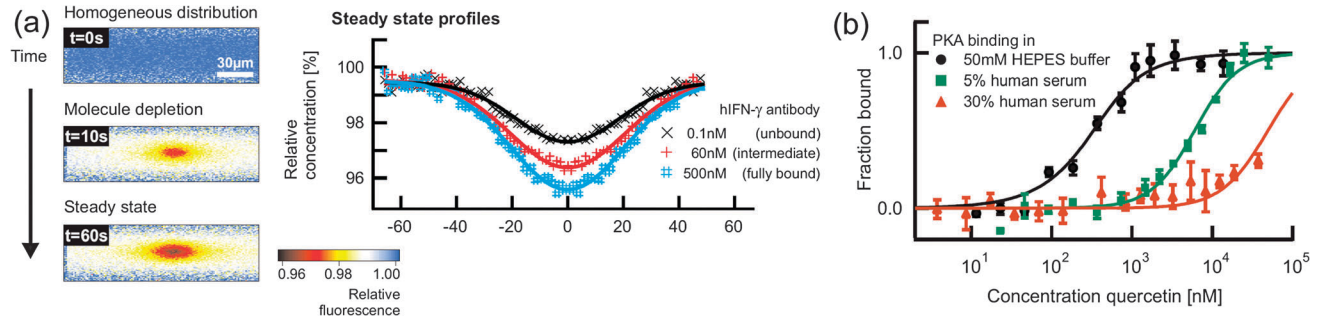

Fig. 9 (a) Microscale thermophoresis for quantification of binding. The thermophoretic depletion depends on the molecule size and linearly reports the binding probability in a binding titration series. The analysis of a concentration series quantifies the dissociation constant K_D. (b) The analysis is specially useful for detecting small molecules in complex biological liquids. An example is the kinase inhibitor quercetin binding to the kinase PKA. We find that the inhibitor significantly binds to the blood protein BSA in serum. [Copyright *Nature Communications*].

Downloaded by Ludwig Maximilians Universitaet Muenchen on 24 January 2011
Published on 17 January 2011 on http://pubs.rsc.org | doi:10.1039/C0CP02359K

The binding shows a clear signal in the Soret coefficient as seen in Fig. 9a. The cAMP dependent kinase PKA was analyzed against the inhibitor quercetin. The kinase was fluorescently labeled and kept at a concentration of 300 nM. The inhibitor quercetin was titrated up to 50 μM in 50 mM HEPES buffer and 5% DMSO (dimethyl sulfoxide). We found an affinity of 130 ± 35 nM, in agreement with literature expectations. The thermophoretic concentration signal changed from 3.8% for the unbound state to 4.53% for the bound state, showing a 19% relative change upon binding of quercetin despite the fact that the bound complex differs by only 1%. We attribute the large signal to changes in the hydration shell originating from water molecules that are either displaced from the binding pocket or reorganized when the protein undergoes conformational changes.

Interestingly, when measured in diluted 5% and 30% blood serum, we found apparent dissociation constants K_D = 6 ± 0.4 μM and 50 ± 7 μM, respectively (Fig. 9b). Subsequent experiments showed that the drop in affinity was due to binding to human serum albumin. This shows that competing interactions, a typical but hard to assess problem in pharmaceutical development, are easily measured with fluorescence-based thermophoresis. In the short time since the development of the technique, a wide range of biological problems have been successfully tackled with the thermophoretic approach.[19,20]

V. An optical conveyor for molecules

The combination of thermophoresis with convection has a long history. Known as thermogravitational column, Clusius and Dickel developed an approach to accumulate molecules in gases in 1938.[37] With the above control of optical fluid flow and optical gradients, we can miniaturize this approach and thus significantly speed it up from several hours down to a mere second. The result is a very flexible optical conveyor for molecules. Its first application showed the concurrent accumulation and replication of DNA molecules in a replication trap. It approaches the replication and selection of genetic molecules in a single chamber, demonstrating two core processes of life in a simple and hydrothermally realistic boundary condition.

The first convection trap for DNA was demonstrated in 2002 using a combination of optically triggered convection and axial thermal gradients.[38] However, it required very low salt conditions and could only significantly trap relatively large DNA molecules with a length of 4000 base pairs. Common to all trap designs is that the thermophoretic depletion is amplified by combining the thermal field with a laser induced perpendicular liquid flow. This method allows us to trap even small DNA molecules in solution.[30,31]

The basic principle is based on a bidirectional flow of the fluid perpendicular to a thermal gradient.[30,31,37,39] As a result, the molecules are pushed by thermophoresis into one side of the flow and are transported preferentially in one direction. Applied to an axially symmetric geometry, freely diffusing molecules in a fluid film are expected to accumulate to a single spot (Fig. 10a). In effect, thermophoresis pushes the molecules to the top, where the water flow shuttles them to the center.

Interestingly, this intricate situation of counterflow and thermal gradient can be created solely by optical means. The thermal gradient is applied by focused infrared absorption in a Chromium-film below the water (Fig. 10b). The bidirectional flow is generated by the movement of the laser spot, based on the thermo-viscous fluid pump which uses thermal expansion in thermally created viscosity gradients, as shown above. We impose an outward flow near the bottom warm side by a radial laser pattern. The counterflow at the top is ensured by mass conservation.

This configuration allows the generation of a bidirectional flow in very thin fluid layers of only 2 μm. With a mean temperature difference of 15 K and a diameter of 200 μm such conveyor belt becomes very efficient even for small polymers with lengths down to 1.5 nm. Fig. 10c shows single stranded oligonucleotides with lengths of 5, 10 and 50 bases, trapped within 3 seconds. The longer DNA molecules are accumulated to higher concentrations and are more tightly confined in the center, with an $1/e$ decay at a radius of 14 μm. By inverting the flow, the conveyor transports the molecules equally efficiently in outward direction as shown for the 1000 base pair DNA in Fig. 10c, 4th image.

The physics of the conveyor belt can be simulated using finite elements. In an axial symmetric geometry we model a bidirectional flow with a maximal speed v_{max} = 200 μm s^{-1}

View Online

Downloaded by Ludwig Maximilians Universitaet Muenchen on 24 January 2011
Published on 17 January 2011 on http://pubs.rsc.org | doi:10.1039/C0CP02359K

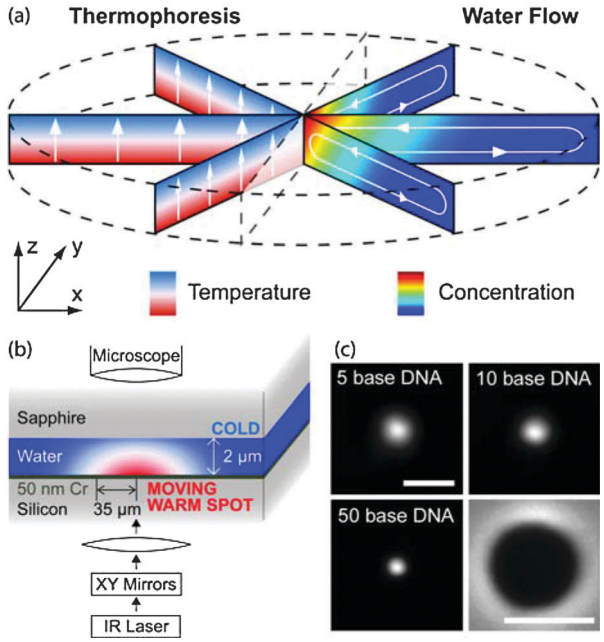

Fig. 10 Conveyor trap. (a) Bio-molecules are efficiently accumulated by a combination of a temperature gradient and perpendicular bidirectional flow. Since thermophoresis predominantly locates the molecules at the colder top, the conveyor-like water flow transports the molecules to the center. (b) Both the temperature gradient and the water flow are generated by a spot of enhanced temperature at the bottom, induced by the laser absorption in a thin metal layer. The water flow is the result of the co-axial thermo-viscous pumping in radial direction. (c) Short DNA is trapped from a diameter of 200 µm within 3 seconds. Longer DNA shows a stronger confinement. The single stranded DNA oligos with lengths of 5, 10 and 50 bases are labeled with the fluorescent dye 6-carboxy-2′,4,4′,5′,7,7′-hexachloro-fluorescein, succinimidyl ester (HEX) to visualize the concentration. By reversing the fluid flow, the molecules are transported off the conveyor, as shown by the 1000 base pair DNA stained with the intercalating dye TOTO-1. Scale bars are 100 µm. [Copyright *Nano Letters*].

within the trapping region $r < 100$ µm. We add the thermophoretic drift $v = S_T D \nabla T$ into the diffusion equation with a temperature gradient ∇T matching temperature imaging measurements using the temperature sensitive dye Cy5. The optical conveyor is simulated for various DNA lengths. Values for the diffusion coefficient D and the Soret coefficient S_T are phenomenologically interpolated. Fig. 11a shows the simulated concentration for the 50 base DNA (color scale). The simulation predicts a two million fold increase of the center concentration in the steady state.

The trapping mechanism transports the particles into the center within 3 seconds. After that period the relative concentration profile inside the trap is equilibrated. To further increase the absolute value of the center concentration, molecules have to diffuse into the region of the trap. To fill the trap up to its steady state concentration, all molecules within a radius of 10 mm would be needed to enter the trap. Fig. 11b shows the measured time trace of the center concentration, compared to the simulation prediction. The two different regimes can be clearly distinguished.

The effective potential depth of the trap can be calculated by assuming a Boltzmann distribution of the DNA molecules in steady state: $U(r) = -kT \ln(c/c_0)$. Fig. 11c shows the simulated shapes of the potentials for 50, 22, 10 and 5 base DNA. The 5 base DNA is expected to be trapped with a potential of 5 kT referring to a 200-fold accumulation. The linear shaped potential results in an exponential distribution of the concentration over the radius of the trap.

The radial fluorescence intensity of trapped DNA molecules is shown in Fig. 11d. The intensities are normalized to the center concentration to compare the accumulation efficiency by the confinement of the distribution for different polymer lengths. The concentration profile differs only in the center of the trap from the expected exponential shape. This is explained by the size of the thermal laser spot with a diameter of $d_{1/e} = 70$ µm which is used to drive the bidirectional fluid flow. In the center the laser spot overlaps and cancels out the flow. This lowers the efficiency of the trap in the center region.

The radial distribution of the measured intensity is fitted with an exponential function in the region beyond $r = 10$ µm. The trapping potential is obtained from the intensity ratio $U_{TRAP}/kT = -\ln(c/c_0) = -\ln[I_{EXP}(0)/I_{FIT}(100\ \mu m)]$, where $I_{EXP}(0)$ is the measured fluorescence intensity in the center. We take the extrapolated intensity at the edge of the trapping region $I_{FIT}(100\ \mu m)$ where the fluorescence measurement is limited by background and the dynamic range of the camera. Fig. 11e shows the measured potential depths of the molecule conveyor for single stranded DNA molecules of different lengths (open circles). The simulated data (solid line) describe the experimental results quantitatively.

Since the conveyor belt is driven entirely optically, its position can be changed easily. Instead of waiting for the molecules to diffuse into the trap, they can be collected while passing over it. Fig. 12a shows 40 nm fluorescent polystyrene beads. Comparable to a vacuum cleaner, the radial conveyor belt collects all particles on the trace. A similar protocol traps 50 base DNA molecules (Fig. 12b).

VI. The replication trap

A biologically interesting extension of the above trap is the combination of the trapping mechanism with a replication mechanism. The ultimate aim is to show that the two central pillars of the Darwinian process, namely replication and selection, are implemented simply by a thermal gradient. On the one hand, the thermal oscillation of the convection flow in a thermal trap gives rise to melting and hybridization cycles of DNA. An already replicated DNA or RNA opens up in the warm side of the chamber and is ready for another cycle of replication. This is the basic principle of the polymerase chain (PCR) reaction. On the other hand, the replicated molecules are selected out and saved from diffusion into the surrounding by the molecular trapping mechanism of combined convection and thermophoresis.

As a first step, we could show the replication and trapping in experiment. We used the replication of DNA using a polymerase protein as the proxy reaction for a replication.[31] In doing so, we implemented the two hallmarks of living matter in a single chamber, namely the replication of genetic

This journal is © the Owner Societies 2011

View Online

Downloaded by Ludwig Maximilians Universitaet Muenchen on 24 January 2011
Published on 17 January 2011 on http://pubs.rsc.org | doi:10.1039/C0CP02359K

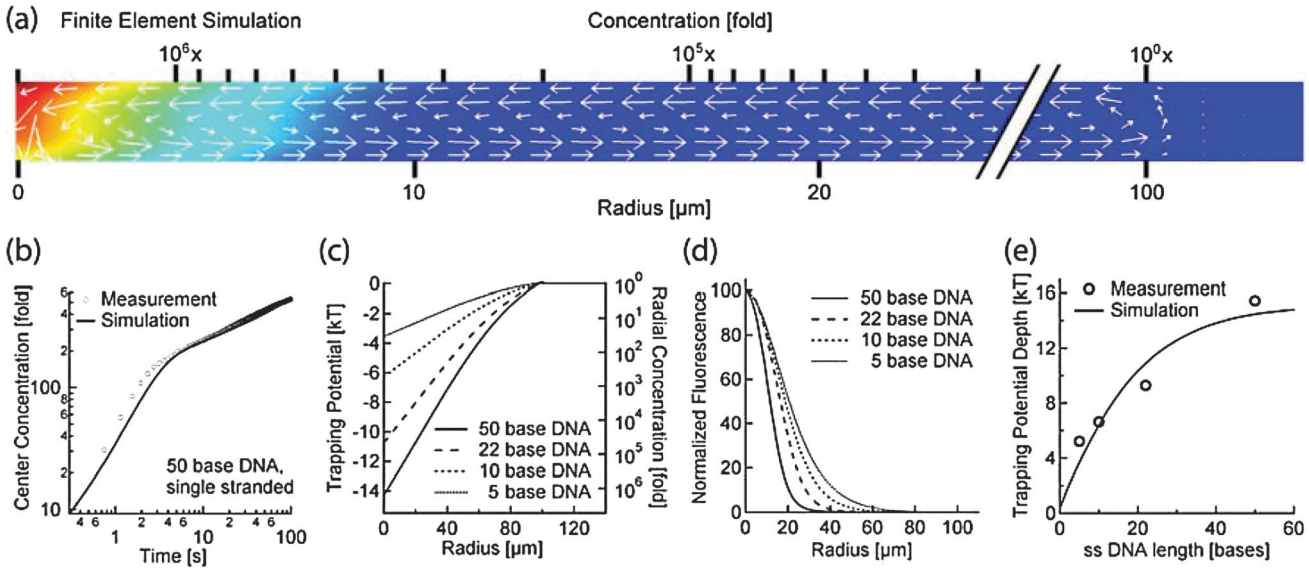

Fig. 11 Theory: (a) Finite element simulation in an axial symmetry confirms the experimental observations and predicts a steady state concentration of 2 million fold for the single stranded 50 base DNA. Arrows represent the fluid flow. (b) Molecules in the trap are shuffled to the center within 3 seconds as shown by the time trace of the center concentration. The successively slower concentration increase refers to diffusion into the region of the trap. The simulation (solid line) confirms the experimental behavior (open circles). (c) Radial distribution of the simulated trapping potential for 5, 10, 22 and 50 base DNA. (d) Measured concentration distribution of the conveyor belt. (e) Measured trapping potential depths for the DNA oligomers (open circles) match finite element simulations (solid line). [Copyright *Nano Letters*].

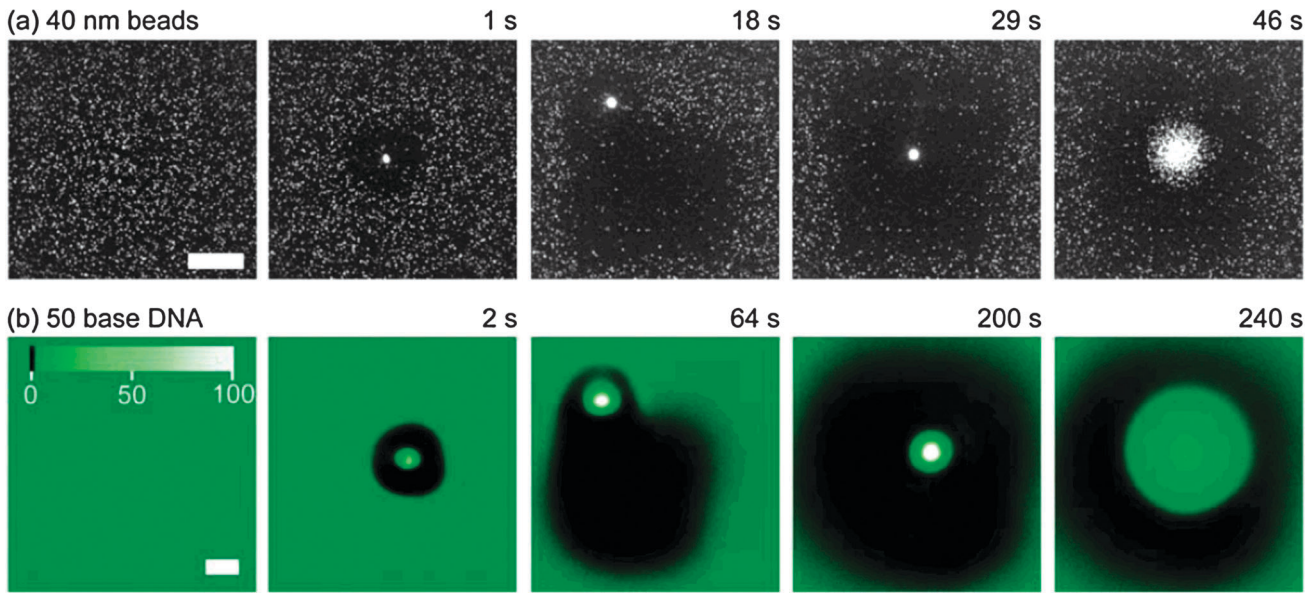

Fig. 12 Moving trap. (a) Since the conveyor belt is driven entirely optically, it can be moved arbitrarily through the solution to collect polystyrene beads with a diameter of 40 nm. After the trap has switched off, the particles diffuse freely. (b) The same processing works for the single stranded 50 base DNA. The color scale is highly nonlinear to visualize both the high concentration in the trapping center and the comparable low contrast between the outside concentration and the depleted area. The scale bars are 100 μm. [Copyright *Nano Letters*].

molecules and their active storage against diffusion. The simple nonequilibrium environment is a thermal gradient. Convective flow drives the DNA replicating polymerase chain reaction while concurrent thermophoresis accumulates the replicated 143 base pair DNA in bulk solution (Fig. 13a). The time constant for accumulation is 92 s while DNA is doubled every 50 s (Fig. 13b).

The experiments explore conditions in pores of a hydrothermal rock which can serve as a model environment for the origin of life. It is possible that such a scheme will be used in the future to select and breed useful DNA or RNA molecules. Interesting is that the setting yields 1700 DNA replications within 24 h, considerably faster than for example *E. coli* with 70 replications per day.

View Online

Downloaded by Ludwig Maximilians Universitaet Muenchen on 24 January 2011
Published on 17 January 2011 on http://pubs.rsc.org | doi:10.1039/C0CP02359K

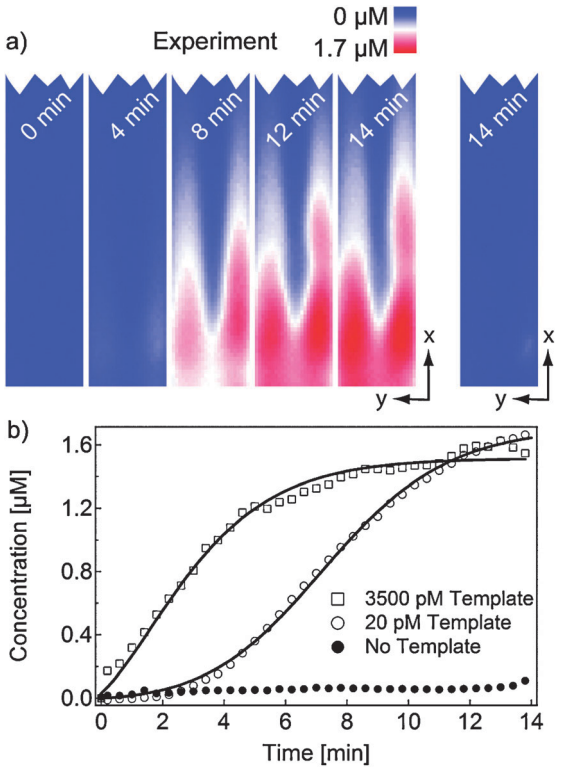

Fig. 13 Replication trap. (a) Fluorescence image of the DNA replicated and accumulated provided by the SYBR green DNA stain. A thermal gradient drives the DNA replication by the temperature oscillation in a thermal convection. The same thermal field selects the replicated DNA by accumulating it at the lower corner of the chamber. Without initial DNA, no replication result is found and fluorescence does not increase above background levels. Such a system mimics the conditions in a rock pore in the vicinity of hydrothermal vents. (b) We record the fluorescence level at the accumulation corner. The DNA replication is exponential and thus a function of its initial concentration. The results are fitted by a combination of the replication and the accumulation dynamics. [Copyright *Physical Review Letters*].

VII. Outlook

We have shown that the optical creation of thermal gradients allows us to control both molecules and water on the microscale. While the optical microflow control has applications in microfluidics, the optical thermophoresis allows the quantification of biomolecule interactions in highly sensitive assays. Both techniques can be combined to trap molecules and to reconstruct conditions for Darwinian evolution using static thermal gradients. As the developments have happened only in the last few years, we expect a number of interesting novel microscale applications using optothermal control in the near future.

Acknowledgements

We thank Natan Osterman for reading the manuscript. Financial support from the NanoSystems Initiative Munich, the International Doctorate Program NanoBioTechnology, and the LMU Initiative Functional Nanosystems is gratefully acknowledged.

References

1 A. Ashkin, Acceleration and trapping of particles by radiation pressure, *Phys. Rev. Lett.*, 1970, **24**, 156.
2 S. M. Block, L. S. B. Goldstein and B. J. Schnapp, Bead movement by single kinesin molecules studied with optical tweezers, *Nature*, 1990, **348**, 348.
3 P. S. Peercy, The drive to miniaturization, *Nature*, 2000, **406**, 1023.
4 A. Ashkin, J. M. Dziedzic, J. E. Bjorkholm and S. Chu, Observation of a single-beam gradient force optical trap for dielectric particles, *Opt. Lett.*, 1986, **11**, 288.
5 S. B. Smith, Y. J. Cui and C. Bustamante, Overstretching B-DNA: The elastic response of individual double-stranded and single-stranded DNA molecules, *Science*, 1996, **271**, 795.
6 R. B. M. Schasfoort, S. Schlautmann, J. Hendrikse and A. van den Berg, Field-effect flow control for microfabricated fluidic networks, *Science*, 1999, **286**, 942.
7 B. Zhao, J. S. Moore and D. J. Beebe, Surface-directed liquid flow inside microchannels, *Science*, 2001, **291**, 1023.
8 B. S. Gallardo, V. K. Gupta, F. D. Eagerton, L. I. Jong, V. S. Craig, R. R. Shah and N. L. Abbott, Electrochemical principles for active control of liquids on submillimeter scales, *Science*, 1999, **283**, 57.
9 M. G. Pollack, R. B. Fair and A. D. Shenderov, Electrowetting-based actuation of liquid droplets for microfluidic applications, *Appl. Phys. Lett.*, 2000, **77**, 1725.
10 D. Psaltis, S. R. Quake and C. Yang, Developing optofluidic technology through the fusion of microfluidics and optics, *Nature*, 2006, **442**, 381.
11 P. Y. Chiou, Z. H. Chang and M. C. Wu, Droplet manipulation with light on optoelectrowetting device, *J. Microelectromech. Syst.*, 2008, **17**, 133.
12 P. Y. Chiou, A. T. Ohta and M. C. Wu, Toward all optical lab-on-a-chip system: optical manipulation of both microfluid and microscopic particles, *Proc. SPIE–Int. Soc. Opt. Eng.*, 2004, **5514**, 73.
13 K. Ladavac and D. Grier, Microoptomechanical pumps assembled and driven by holographic optical vortex arrays, *Opt. Express*, 2004, **12**, 1144.
14 A. A. Darhuber, J. M. Davis, S. M. Troian and W. W. Reisner, Thermocapillary actuation of liquid flow on chemically patterned surfaces, *Phys. Fluids*, 2003, **15**, 1295.
15 A. Wixforth, C. Strobl, C. Gauer, A. Toegl, J. Scriba and Z. v. Guttenberg, Acoustic manipulation of small droplets, *Anal. Bioanal. Chem.*, 2004, **379**, 982.
16 F. M. Weinert, J. A. Kraus, T. Franosch and D. Braun, Microscale Fluid Flow Induced by Thermoviscous Expansion Along a Traveling Wave, *Phys. Rev. Lett.*, 2008, **100**, 164501.
17 F. M. Weinert and D. Braun, Optically driven fluid flow along arbitrary microscale patterns using thermoviscous expansion, *J. Appl. Phys.*, 2008, **104**, 104701.
18 F. M. Weinert, M. Wühr and D. Braun, Light driven microflow in ice, *Appl. Phys. Lett.*, 2009, **94**, 113901.
19 P. Baaske, C. J. Wienken, P. Reineck, S. Duhr and D. Braun, Optical Thermophoresis for Quantifying the Buffer Dependence of Aptamer Binding, *Angew. Chem., Int. Ed.*, 2010, **49**, 2238.
20 C. J. Wienken, P. Baaske, U. Rothbauer, D. Braun and S. Duhr, Protein Binding Assays in Biological Liquids using Microscale Thermophoresis, *Nat. Commun.*, 2010, **1**, 100.
21 M. Giglio and A. Vendramini, Soret-Type Motion of Macromolecules in Solution, *Phys. Rev. Lett.*, 1977, **38**, 26.
22 C. Debuschewitz and W. Köhler, Molecular Origin of Thermal Diffusion in Benzene + Cyclohexane Mixtures, *Phys. Rev. Lett.*, 2001, **87**, 055901.
23 J. Rauch and W. Köhler, Diffusion and Thermal Diffusion of Semidilute to Concentrated Solutions of Polystyrene in Toluene in the Vicinity of the Glass Transition, *Phys. Rev. Lett.*, 2002, **88**, 185901.
24 R. Piazza and A. Guarino, Soret Effect in Interacting Micellar Solutions, *Phys. Rev. Lett.*, 2002, **88**, 208302.
25 R. Rusconi, L. Isa and R. Piazza, Thermal-lensing measurement of particle thermophoresis in aqueous dispersions, *J. Opt. Soc. Am. B*, 2004, **21**, 605.
26 S. A. Putnam and D. G. Cahill, Transport of Nanoscale Latex Spheres in a Temperature Gradient, *Langmuir*, 2005, **21**, 5317–5323.

 This journal is © the Owner Societies 2011

View Online

27 S. Duhr and D. Braun, Why molecules move along a temperature gradient, *Proc. Natl. Acad. Sci. U. S. A.*, 2006, **103**, 19678.
28 S. Duhr and D. Braun, Optothermal Molecule Trapping by Opposing Fluid Flow with Thermophoretic Drift, *Phys. Rev. Lett.*, 2006, **97**, 038103.
29 F. M. Weinert and D. Braun, Observation of Slip Flow in Thermophoresis, *Phys. Rev. Lett.*, 2008, **101**, 168301.
30 F. M. Weinert and D. Braun, An optical conveyor for molecules, *Nano Lett.*, 2009, **9**, 4264.
31 C. B. Mast and D. Braun, Thermal Trap for DNA Replication, *Phys. Rev. Lett.*, 2010, **104**, 188102.
32 H.-R. Jiang, H. Wada, N. Yoshinaga and M. Sano, Manipulation of Colloids by Nonequilibrium Depletion Force in a Temperature Gradient, *Phys. Rev. Lett.*, 2009, **102**, 208301.
33 P. Reineck, C. J. Wienken and D. Braun, Thermophoresis of single stranded DNA, *Electrophoresis*, 2010, **31**, 279–286.
34 M. Braibanti, D. Vigolo and R. Piazza, Does Thermophoretic Mobility Depend on Particle Size?, *Phys. Rev. Lett.*, 2008, **100**, 108303.
35 J. Morthomas and A. Würger, Thermoelectric effect on charged colloids in the Hückel limit, *Eur. Phys. J. E*, 2008, **27**, 425–434.
36 D. Vigolo, S. Buzzaccaro and R. Piazza, Thermophoresis and Thermoelectricity in Surfactant Solutions, *Langmuir*, 2010, **26**, 7792–7801.
37 K. Clusius and G. Dickel, Neues Verfahren zur Gasentmischung und Isotopentrennung, *Naturwissenschaften*, 1938, **26**, 546.
38 D. Braun and A. Libchaber, Trapping of DNA by thermophoretic depletion and convection, *Phys. Rev. Lett.*, 2002, **89**, 188103.
39 P. Baaske, F. M. Weinert, S. Duhr, K. H. Lemke, M. J. Russell and D. Braun, Extreme accumulation of nucleotides in simulated hydrothermal pore systems, *Proc. Natl. Acad. Sci. U. S. A.*, 2007, **104**, 9346.

Downloaded by Ludwig Maximilians Universitaet Muenchen on 24 January 2011
Published on 17 January 2011 on http://pubs.rsc.org | doi:10.1039/C0CP02359K